Introductory Lectures on Collider Physics

TIM M. P. TAIT

Department of Physics & Astronomy,
University of California,
Irvine, CA 92697 USA
E-mail: ttait@uci.edu

LIAN-TAO WANG

Department of Physics,
Enrico Fermi Institute,
University of Chicago,
Chicago, IL 60637, USA
E-mail: liantaow@uchicago.edu

The Dark Secrets of the Terascale Downloaded from www.worldscientific.com
by MONASH UNIVERSITY on 04/16/16. For personal use only.

These are elementary lectures about collider physics.* They are aimed at graduate students who have some background in computing Feynman diagrams and the Standard Model, but assume no particular sophistication with the physics of high energy colliders.

1. Introduction

High energy colliders are currently our most powerful tools providing information about short distance physics. With the LHC now gathering data in earnest, this is a very exciting time with huge potential for new discoveries that may transform our view of physics at the electroweak scale. Understanding how to make predictions and understand the experimental results will be an essential part of those discoveries. These notes aim to provide a (very) elementary introduction to some of the key concepts, hopefully providing a launching pad for learning from more sophisticated treatments.

They are similar in philosophy to three very nice lectures about collider physics given by T. Han, T. Plehn and M. Perelstein at previous years of the TASI summer school[1–3] While the similarities between these reviews

*This version is mainly based on TT's lecture for the ICTP summer school on particle physcs in June of 2011. An expanded version will appear soon.

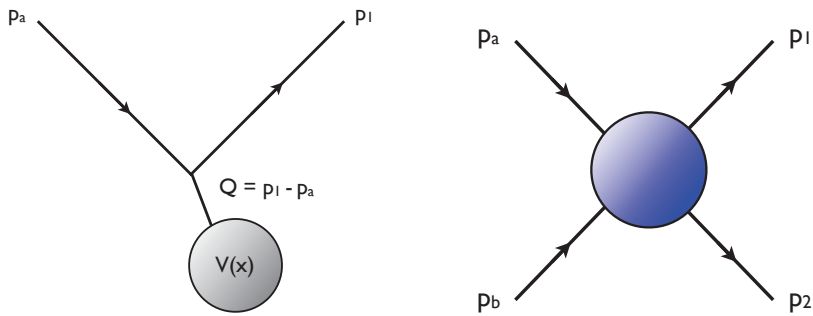

Fig. 1. Left: a particle scattering off of an external potential. Right: Two particles scattering.

The Dark Secrets of the Terascale Downloaded from www.worldscientific.com by MONASH UNIVERSITY on 04/16/16. For personal use only.

are largely the result of convergent evolution (of thoughts), I did benefit in polishing these lectures from the previous ones, and readers interested in more detail than I was able to provide here and/or alternative perspectives are highly encouraged to read them as well.

2. Kinematics

Let's begin by reminding ourselves of what we all learned back in ordinary quantum mechanics. If we want to study a potential $V(\vec{x})$ by scattering some kind of particle a off of it, we prepare a beam of particles with four-momentum p_a, and measure their out-going (scattered) four momenta p_1 (see Figure 1a). The 4-vector $Q \equiv p_1 - p_a$ describes the momentum transfer in each reaction, and the amplitude for scattering for a given Q is given by the Fourier transform of V:

$$\mathcal{A}(Q) \propto \int d^3\vec{x} \;\; e^{i\vec{q}\cdot\vec{x}} \;\; V(\vec{x}) \; . \tag{1}$$

Since large values of $|\vec{q}|$ correspond to small distances, the large $|\vec{q}|$ events provide information about small structure in V.

Most often in particle physics, we are more interested in the short distance physics of another particle. We can replace $V(x)$ with another particle b, and study the $2 \to 2$ reaction,

$$p_a + p_b \to p_1 + p_2 \; , \tag{2}$$

(see Figure 1b) in which case we simultaneously study the short distance interactions between a and b in the large $Q \equiv p_1 - p_a$ regime. In fact, particles 1 and 2 need not even be the same as a and b, so for high enough

The Dark Secrets of the Terascale Downloaded from www.worldscientific.com by MONASH UNIVERSITY on 04/16/16. For personal use only.

energies we may succeed at producing new particles we have never seen before. In any case, energy-momentum conservation implies,

$$p_a + p_b = p_1 + p_2 \ . \tag{3}$$

It is easy to choose any coordinate system we like by applying Lorentz transformations to all four of the momenta. In practice, a convenient choice is the center of momentum (CoM) frame, in which $\vec{p}_a = -\vec{p}_b$. Since these momenta define a line (and nothing in the initial state distinguishes anything going on in the transverse directions,[a] we can always choose the axis defined by $\vec{p}$ to be the $\hat{z}$-axis. In this case, we can write the 4-momenta of the incoming particles,

$$\begin{aligned} p_a &\equiv (E_a, 0, 0, p) \\ p_b &\equiv (E_b, 0, 0, -p) \end{aligned} \tag{4}$$

where $E_a \equiv \sqrt{p^2 + m_a^2}$ and $E_b \equiv \sqrt{p^2 + m_b^2}$ so the particles are on-shell. An important thing to notice is that the quantity p completely specifies the momenta of the initial state (if our particles have spins we should also define their components along $\hat{z}$). We can encode this information in a Lorentz-invariant way by defining the Mandelstam s variable,

$$s \equiv (p_a + p_b)^2 = (p_1 + p_2)^2 = (E_a^{CoM} + E_b^{CoM})^2 \tag{5}$$

where the second equality follows from energy conservation and the last emphasizes that these are related to the initial energies in the center of mass frame. That final expression makes it obvious that $s \geq (m_a + m_b)^2$ and it should also be clear that $s \geq (m_1 + m_2)^2$.

Now let's discuss the final state particles 1 and 2. In the CoM frame, they must have equal and opposite spatial momenta, since $p_a + p_b$ has only a time-component by construction in that frame. We can always choose our $\hat{x}$-axis to lie in the plane formed by $\vec{p}_1$ and $\vec{p}_a$, and we can write the four-momenta as,

$$\begin{aligned} p_1 &\equiv (E_1,\ p's_\theta, 0,\ p'c_\theta) \\ p_2 &\equiv (E_2, -p's_\theta, 0, -p'c_\theta) \end{aligned} \tag{6}$$

where $E_1 \equiv \sqrt{p'^{\,2} + m_1^2}$ and $E_2 \equiv \sqrt{p'^{\,2} + m_2^2}$ and I have introduced the short-hand notation $s_\theta \equiv \sin\theta$ and so on. Energy conservation tells us that

[a]Including spins: since we can measure at most one component of the spin (if any) of a and b, we can choose the spin measurement axis to also be the $\hat{z}$-axis.

$E_1 + E_2 = E_a + E_b$, or written out as functions of p and p', that the magnitude p' is determined entirely by p and the four masses. Thus, p' will always turn out the same in a $2 \to 2$ reaction involving the same particles and fixed p, and the final state is defined by the scattering angle θ and the (trivial) azimuthal angle ϕ which defines the orientation of the $\hat{x}$-axis.

We can encode the dependence on the scattering angle θ in a Lorentz invariant,

$$\begin{aligned} t \equiv (p_1 - p_a)^2 = (p_b - p_2)^2 &= m_1^2 + m_a^2 - 2p_1 \cdot p_a \\ &= m_1^2 + m_a^2 - 2(E_a^{CoM} E_1^{CoM} - pp' \cos\theta) \ . \end{aligned} \tag{7}$$

Needless to say, if we know s and t, we know everything interesting about the momenta involved in a $2 \to 2$ reaction. Notice that $t = Q^2$ from our earlier discussion, and it tells us about the 4-momentum transfer and the distance scale being probed.

The physical range of t can be easily determined by remembering that $-1 \leq c_\theta \leq +1$. Thus, we have:

$$t_1 \leq t \leq t_0 \ , \tag{8}$$

where,

$$t_{0,1} = \left(\frac{m_a^2 - m_1^2 - m_b^2 + m_2^2}{2\sqrt{s}} \right)^2 - (p \mp p')^2. \tag{9}$$

For very high energy reactions (all energies much larger than all masses):

$$\begin{aligned} p_a &\to (\sqrt{s}/2, 0, 0, \sqrt{s}/2) \\ p_b &\to (\sqrt{s}/2, 0, 0, -\sqrt{s}/2) \\ p_1 &\to (\sqrt{s}/2, \sqrt{s}/2 s_\theta, 0, \sqrt{s}/2 c_\theta) \\ p_2 &\to (\sqrt{s}/2, -\sqrt{s}/2 s_\theta, 0, -\sqrt{s}/2 c_\theta) \end{aligned}$$

and the limits on t become $t_0 \to 0$ and $t_1 \to -s$. This helps make it clear why we need high energies to probe short distances: it is not enough to have high energy (large s), but we need high energy to reach large values of t, for which we have wide angle scattering which probes short distances.

Before closing the section on kinematics, I should mention that some people define a third Mandelstam invariant,

$$u \equiv (p_1 - p_b)^2 = (p_a - p_2)^2 \ . \tag{10}$$

Since it is redundant with s and t, we have a relation among the three:

$$s + t + u = m_a^2 + m_b^2 + m_1^2 + m_2^2 \ . \tag{11}$$

The Dark Secrets of the Terascale Downloaded from www.worldscientific.com by MONASH UNIVERSITY on 04/16/16. For personal use only.

The Dark Secrets of the Terascale Downloaded from www.worldscientific.com by MONASH UNIVERSITY on 04/16/16. For personal use only.

3. Cross Sections

If we are looking for events of some kind, we can write the rate at which they occur in a way which is independent of how we prepare the initial particles going into the reaction in terms of the cross section σ,

$$N = \sigma \; L \; \epsilon \tag{12}$$

where N is the number of events observed, σ is the cross section for the reaction, typically measured in barns ($1 \text{ bn} = 10^{-24}\text{cm}^2$) or GeV^{-2}. $L \equiv \int dt \; \mathcal{L}$ is the integrated luminosity, which represents how much collision data was collected, and can be expressed in barn^{-1} or GeV^2. Finally, ϵ is a dimensionless number that represents the fact that particle detectors typically have a limited efficiency to record every particle produced. In practice, ϵ is something the experimentalists need to determine for themselves (and then tell to the world when they commission their detectors). L is determined by how long the accelerator was running and collecting data.

To compute a cross section, we compute the matrix element squared ($|\mathcal{M}|^2$) for the quantum transition of interest, and we sum over the allowed final states,

$$d\sigma = \frac{1}{2s} \left(\prod_{i=1}^{N} \frac{d^3\vec{p}_i}{(2\pi)^3} \frac{1}{2E_i} \right) (2\pi)^4 \; \delta^{(4)}(p_a + p_b - \sum_i p_i) \; |\mathcal{M}(p_a, p_b \to \{p_i\})|^2 \tag{13}$$

where the first factor corrects for the flux of the incoming (treated as massless) particles, and the 4-delta function enforces energy momentum conservation. If our particles have spins, we can specify them as part of $\mathcal{M}$, or (more often) we cannot prepare the spin of the initial state or measure the spins of the final state. In such cases, we sum over the final spins and average over the initial ones. We call the matrix element squared after this operation $\overline{|\mathcal{M}|^2}$. In these lectures, we will always be interested in these summed/averaged matrix elements.

Note that we wrote $d\sigma$ in the CoM frame, but it is invariant under boosts along the beam axis, so we will rarely have to worry about that fact. Also notice that each final state particle has 3 independent momentum components, for $3N$ total. Since there are 4 energy-momentum constraints, the total number of independent quantities is $3N - 4$. In a $2 \to 2$ reaction, these would be the θ and ϕ angles describing the final state momenta, where we previously ignored ϕ because we knew the matrix element cannot possibly depend on it.

The Dark Secrets of the Terascale Downloaded from www.worldscientific.com by MONASH UNIVERSITY on 04/16/16. For personal use only.

3.1. *Phase Space Recursion*

There is a very useful way to rewrite the phase space integrals for complicated many-particle final states in terms of a two particle final state like the ones we discussed in Section 2. First, let's introduce some more compact notation. We can represent the phase space measure for a given particle i by,

$$d\Pi_i \equiv \frac{d^3\vec{p}_i}{(2\pi)^3}\frac{1}{2E_i} \tag{14}$$

from which we can build the n-body (particle) phase space,

$$d\Phi_n(P; p_1, ...p_n) \equiv (2\pi)^4\ \delta\left(P - \sum_i p_i\right)\ \prod_{i=1}^{N} d\Pi_i \tag{15}$$

where P is the incoming 4-momentum ($p_a + p_b$ in our previous discussion). Our useful identity is,

$$d\Phi_n(P; p_1, ..., p_n) = d\Phi_{n-j+1}(P; p_{j+1}, ...p_n)\ \ d\Phi_j(q; p_1, ...p_j)\ \ \frac{dq^2}{(2\pi)}\ , \tag{16}$$

which in effect takes the whole n-particle phase space and splits it into the phase space to produce particles $j+1$ through n plus a fictitious particle q, followed by the "decay" of q into particles 1 through j. Since q is just a way to think about splitting the integration up into smaller pieces, we should integrate over all possible values of the fictitious mass^2, q^2.

We will make use of this expression for $n = 3$ (and $j = 2$) when we discuss $e^+e^- \to q\bar{q}g$ below. One immediate place where we can see the utility of this kind of decomposition would be when we have intermediate particles which are close to on-shell inside our matrix elements. As we will see when we discuss resonances below, such cases will have matrix elements which can often be approximated as containing δ-functions in q^2. Rewriting the full phase space this way allows us to easily perform the integration over q^2 and get some intuition for what the (otherwise in general complicated) momenta typically look like in such a reaction.

4. $e^+e^- \to \mu^+\mu^-$

Let's think about $e^+e^- \to \mu^+\mu^-$. Since $m_\mu \sim 200 \times m_e$, if we have enough energy to make muons in the first place, it must be a reasonably good approximation to drop m_e compared to either m_μ or $\sqrt{s}$. So we will treat the electron (but not, for now, the muon) as massless.

The Dark Secrets of the Terascale Downloaded from www.worldscientific.com by MONASH UNIVERSITY on 04/16/16. For personal use only.

Applying our formula for the cross section, Eq. (13),

$$d\sigma = \frac{1}{8\pi^2 s}\,\frac{|\vec{p_1}|^2 d|\vec{p_1}|}{2E_1} d\Omega_1\,\frac{|\vec{p_2}|^2 d|\vec{p_2}|}{2E_2} d\Omega_2\;\delta^{(4)}(p_a+p_b-p_1-p_2)\;\overline{|\mathcal{M}|^2} \quad (17)$$

where $d\Omega_i \equiv d\cos\theta_i d\phi_i$ and we'll discuss $\overline{|\mathcal{M}|^2}$ at length later on. For now let's focus on the kinematics.

The 3 spatial pieces of the delta function require:

$$\begin{aligned} |\vec{p_2}| &= |\vec{p_1}| \equiv p \\ \theta_2 &= -\theta_1 \\ \phi_2 &= \pi + \phi_1 \end{aligned} \quad (18)$$

and we can use those three factors to do the $d^3\vec{p}_2$ integration, with the understanding that we replace $\vec{p}_2 \to -\vec{p}_1$ inside the matrix element as well as in E_2, which is now equal to E_1 as a result. We arrive at,

$$d\sigma = \frac{1}{2s}\frac{1}{(2\pi)^2}\,\frac{p^2}{4E_1^2}\;\delta(E_a+E_b-E_1-E_2)\;\overline{|\mathcal{M}|^2}\;\; d\Omega_1 dp\;. \quad (19)$$

To use the remaining delta function, it is useful to change the integration over dp into one over dE. That is easily accomplished by noting that $E = \sqrt{p^2+m^2}$, so:

$$dE = \frac{p}{E}dp\;. \quad (20)$$

We will also make use of the CoM frame for which $E_a + E_b = \sqrt{s}$. Thus,

$$d\sigma = \frac{1}{2s}\frac{1}{(2\pi)^2}\frac{p(E_1)}{4E_1}\;\overline{|\mathcal{M}|^2}\;\delta(\sqrt{s}-2E_1)d\Omega_1 dE_1 \quad (21)$$

$$d\sigma = \frac{1}{32\pi^2 s}\frac{p(E_1)}{\sqrt{s}}\;\overline{|\mathcal{M}|^2}\;d\Omega\;. \quad (22)$$

Since ϕ_1 is trivial ($\overline{|\mathcal{M}|^2}$ does not depend on it), we may as well integrate over it, which physically just means that we will accept any event where $e^+e^- \to \mu^+\mu^-$ independently from what value ϕ_1 happens to take. The last thing to notice is that by changing variables from dp to dE_1, p has become a function of E_1:

$$p(E_1) = \sqrt{E_1^2 - m^2} = \sqrt{\frac{s}{4} - m^2} = \frac{\sqrt{s}}{2}\sqrt{1-\frac{4m^2}{s}} \quad (23)$$

where one often sees the definition $\beta = \sqrt{1-4m^2/s}$ used in the literature. Altogether, this leads us to,

$$\frac{d\sigma}{d\cos\theta} = \frac{1}{32\pi s}\sqrt{1-\frac{4m^2}{s}}\;\overline{|\mathcal{M}|^2}(s,\theta)\;. \quad (24)$$

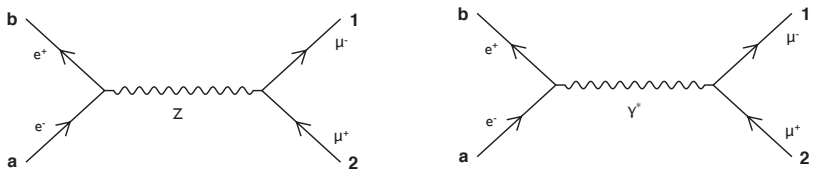

Fig. 2. Feynman diagrams at leading order for $e^+e^- \to \mu^+\mu^-$ in the Standard Model.

The Dark Secrets of the Terascale Downloaded from www.worldscientific.com by MONASH UNIVERSITY on 04/16/16. For personal use only.

Of course, all of the interesting stuff is actually the s and θ dependence of $\overline{|\mathcal{M}|^2}$, and we will discuss this next.

In the Standard Model (SM), there are two Feynman diagrams contributing to the reaction $e^+e^- \to \mu^+\mu^-$ at leading order in perturbation theory (see Figure 2). They correspond to exchange of a virtual photon (γ^*) or Z-boson, respectively. To start out, let's take $\sqrt{s} \ll M_Z$. In this limit, the Z exchange graph is suppressed compared to the photon graph, so we can approximate the whole answer as the photon result,

$$-i\mathcal{M} = [\bar{u}_1 ie\gamma^\mu v_2] \frac{-ig_{\mu\nu} + ...}{s} [\bar{v}_b ie\gamma^\nu u_a] \ , \tag{25}$$

where e is the QED gauge coupling and the ... include terms which drop out in the limit of zero electron mass. Squared and averaged/summed over initial/final spins, this is:

$$\overline{|\mathcal{M}|^2} = \frac{e^4\left(s+2m^2\right)}{s^2}\left(1+\cos^2\theta\right) \ . \tag{26}$$

Thus,

$$\frac{d\sigma}{d\cos\theta} = \frac{\pi\alpha^2}{2s}\frac{s+2m^2}{s}\sqrt{1-\frac{4m^2}{s}}\left(1+\cos^2\theta\right) \ , \tag{27}$$

where $\alpha \equiv e^2/(4\pi)$ is the usual fine structure constant. This expression indicates that muons tend to be produced more in both the forward and backward directions, as shown in Figure 3a. If we integrate this expression over $\cos\theta$, we arrive at the dependence of the inclusive cross section on the initial energy s,

$$\sigma(s) = \int_{-1}^{+1} d\cos\theta \frac{d\sigma}{d\cos\theta} = \frac{4\pi\alpha^2(s+2m^2)}{3s^2}\sqrt{1-\frac{4m^2}{s}} \ . \tag{28}$$

This function is plotted in Figure 3b, which shows the sharp turn-on at $s \simeq 4m_\mu^2$ and subsequent fall as $1/s$ at large energies.

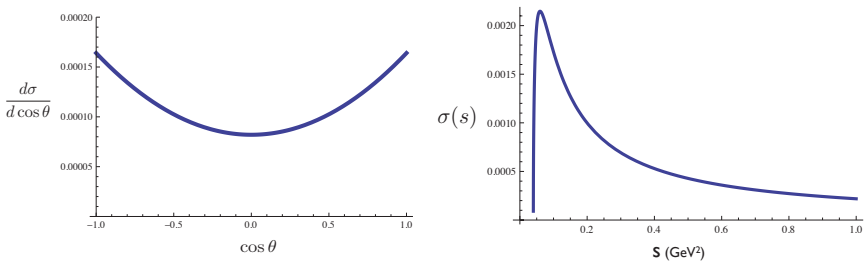

Fig. 3. Distribution of $d\sigma/d\cos\theta$ in $e^+e^- \to \mu^+\mu^-$ as well as the dependence of the inclusive cross section on the incoming energy, $\sigma(s)$.

The Dark Secrets of the Terascale Downloaded from www.worldscientific.com by MONASH UNIVERSITY on 04/16/16. For personal use only.

Homework: Derive the θ and energy dependence for production of *scalar* muons, $e^+e^- \to \tilde{\mu}^+\tilde{\mu}^-$. In reality, scalar muons must be heavy enough that it is not a good approximation to neglect the Z boson, but neglect it anyway. You should find a differential cross section proportional to $\sin^2\theta$.

The results of the exercise illustrate an important point. Though we cannot directly measure the spin of the final state particles, we can sometimes infer them through the kinematic distributions. In this case, the key is that the intermediate particle (photon) is spin-1. As a result, we can track the flow of angular momentum through the two processes:

$$\begin{array}{ccccc} e^+e^- & \to & \gamma^* & \to & \mu^+\mu^- \\ S=1 & & S=1 & & S=1 \end{array} \quad \text{versus} \quad \begin{array}{ccccc} e^+e^- & \to & \gamma^* & \to & \tilde{\mu}^+\tilde{\mu}^- \\ S=1 & & S=1 & & L=1 \end{array}$$

The intermediate photon requires angular momentum $J = 1$. For ordinary muons, as fermions, this is most easily realized in the s-wave ($L = 0$) for an $S = 1$ spin state. For scalar muons, there is no spin to make up $J = 1$, and we are forced to go to an $L = 1$ (p-wave) configuration, with different angular and threshold energy dependence.

It is worth mentioning in passing that the process $e^+e^- \to$ hadrons begins at lowest order at energies far below the Z boson mass with exactly the same photon exchange, with quarks in the final state (since gluons carry no electric charge they cannot be produced at lowest order in perturbation theory) instead of muons, and the replacement of the muon electric charge by the quark charge, effectively multiplying the cross section by $N_c \sum Q_q^2$, where $Q = +2/3$ for the up-type quarks and $-1/3$ for the down-type quarks

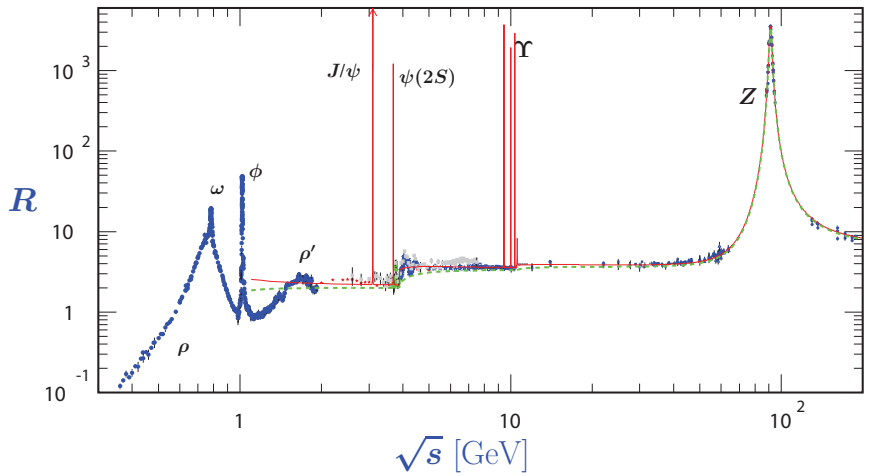

Fig. 4. The ratio of production of hadrons in e^+e^- annihilations to production of muons, as a function of the center-of-mass energy, and for a variety of high energy experiments, from.[5]

and $N_c = 3$ counts the three colors of each quark. We'll say more about this below in Section 5, but for now let's note an important point: just being able to produce new particles already can lead us to discover them! In fact, both the charm and bottom quarks were discovered by looking at the process $e^+e^- \to$ hadrons as a function of energy. If we define a quantity normalized to the muon rate,

$$R \equiv \frac{e^+e^- \to \text{ hadrons}}{e^+e^- \to \mu^+\mu^-} \ . \tag{29}$$

It effectively just counts the number of quarks we have enough energy to produce, weighted by their electric charge squared. In Figure 4 we see a plot of experimental data for this ratio, including the jumps it experiences when the collider has enough energy to produce pairs of charm or bottom quarks.

Now let's go back to the Z-exchange diagram. It looks a lot like the photon graph, with the difference that the Z itself has a non-zero mass and the couplings to electrons and muons are chiral (meaning: they couple differently to left- and right-handed fermions). We will assume that the Z couplings to electrons and muons are equal, as is predicted by the Standard

The Dark Secrets of the Terascale Downloaded from www.worldscientific.com by MONASH UNIVERSITY on 04/16/16. For personal use only.

Model and verified to exquisite accuracy.[4] The matrix element is,

$$-i\mathcal{M} = \left[\bar{u}_1 i\gamma^\mu \left(g_R P_R + g_L P_L\right) v_2\right] \frac{-ig_{\mu\nu} + ...}{s - M_Z^2} \left[\bar{v}_b i\gamma^\nu \left(g_R P_R + g_L P_L\right) u_a\right] \ , \tag{30}$$

where $P_{L/R}$ are the left-handed/right-handed projectors and once again the ... refer to terms that vanish for the massless electrons. We can see from the propagator denominator that this graph will get very large when $s \simeq M_Z^2$, which will allow us to neglect both the muon mass and the photon exchange contribution for such energies.

In fact, things seem problematic for $s \simeq M_Z^2$ – the amplitude not only becomes large, but seems to be infinite right at M_Z^2. Such behavior is obviously unphysical. In fact, it is an artifact of our working to leading order in perturbation theory. At the next-to-leading order, the denominator of the propagator picks up an imaginary part,

$$G^{-1}(p^2) = p^2 - M_Z^2 + iM_Z\Gamma_Z \tag{31}$$

from diagrams such as those shown in Figure 5. (That Feynman graph also corrects the real part of the propagator, and those corrections turn out to be UV divergent, and require both mass and wave function renormalization – but the imaginary part is finite). The optical theorem relates the imaginary part of the loop amplitude to the intermediate particles going onto their mass shells, and thus is guaranteed to produce the actual decay width.[b] Having included the imaginary part of the propagator, $\overline{|\mathcal{M}|^2}$ is now proportional to,

$$\overline{|\mathcal{M}|^2} \propto \frac{1}{\left(s - M_Z^2\right)^2 + M_Z^2\Gamma_Z^2} \ , \tag{32}$$

the famous Breit-Wigner function (see figure 6).

The chiral couplings of the Z lead to a more interesting angular dependence:

$$\overline{|\mathcal{M}|^2} = \frac{s}{\left(s - M_Z^2\right)^2 + M_Z^2\Gamma_Z^2} \times \left\{\left(g_L^2 + g_R^2\right)^2 \left(1 + \cos^2\theta\right) + 2\left(g_L^2 - g_R^2\right)^2 \cos\theta\right\} \tag{33}$$

[b]You can find a much more detailed discussion along with many models of resonances discussed in my lectures at TASI-08.[6] A copy of these lectures should be posted as supplementary information on the school website, and can also be obtained from my UCI home page. Note that they are aimed at a slightly higher level than these lectures!

The Dark Secrets of the Terascale Downloaded from www.worldscientific.com by MONASH UNIVERSITY on 04/16/16. For personal use only.

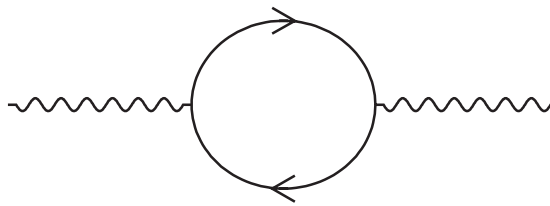

Fig. 5. First order correction to the Z propagator from a loop of fermions.

The Dark Secrets of the Terascale Downloaded from www.worldscientific.com by MONASH UNIVERSITY on 04/16/16. For personal use only.

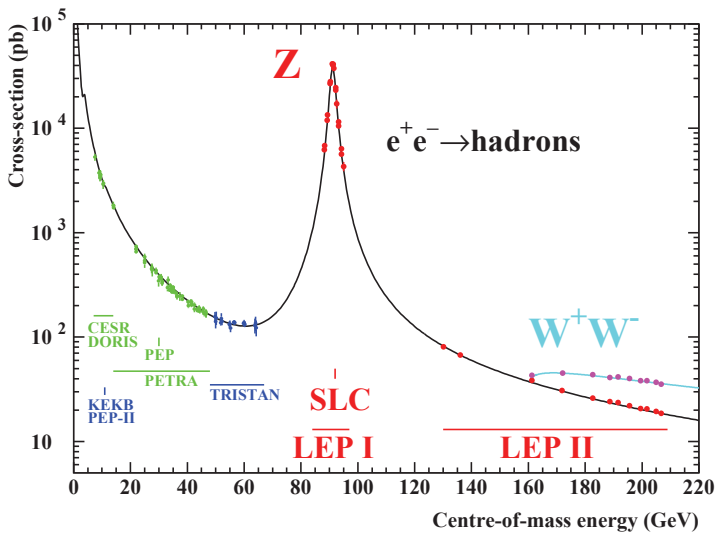

Fig. 6. The rate for $e^+e^- \to$ hadrons as a function of the CoM energy, including measurements from several experiments.[7]

which we can use to separately extract $|g_L|^2$ and $|g_R|^2$ by studying the angular distributions of the outgoing muons from Z decays. Let's see how this works.

LEP produced millions of approximately on-shell Z bosons through e^+e^- annihilation. From here, one easy quantity to derive is the number of $Z \to \mu^+\mu^-$ decays divided by the number of $Z \to$ hadron decays,

$$R_\mu \equiv \frac{e^+e^- \to Z \to \mu^+\mu^-}{e^+e^- \to Z \to \text{ hadrons}} \tag{34}$$

It is somewhat amusing that $R_\mu = 1/R$ in terms of the quantity we looked at before at lower energies to discover the c and b quarks. Since this quan-

tity accepts muons no matter at which θ they are produced, we integrate $d\sigma/d\cos\theta$ over $\cos\theta$. The term proportional to $\cos\theta$ integrates away, and we are left with a prediction for R_μ:

$$R_\mu = \frac{({g_L^\mu}^2 + {g_R^\mu}^2)}{\sum_q ({g_L^q}^2 + {g_R^q}^2)} \ , \tag{35}$$

which measures the sum of the muon couplings squared relatively the sum over couplings to all quarks which are light enough to appear in a Z boson decay: u, d, s, c, and b.

A second useful quantity to measure is the "forward-backward asymmetry", which measures the number of muons which go forward ($\cos\theta > 0$) compared to the number which go backward ($\cos\theta < 0$),

$$A_{FB}^\mu = \frac{N_F - N_B}{N_F + N_B} \tag{36}$$

Taking our differential cross section and performing the integrals results in,

$$A_{FB}^\mu = \frac{3}{4} \frac{({g_L^\mu}^2 - {g_R^\mu}^2)}{({g_L^\mu}^2 + {g_R^\mu}^2)} \frac{({g_L^e}^2 - {g_R^e}^2)}{({g_L^e}^2 + {g_R^e}^2)} \tag{37}$$

where just to make a point, we have separated out the electron from the muon couplings, despite their being equal in the SM. We sometimes define the asymmetry

$$A_\mu = \frac{({g_L^\mu}^2 - {g_R^\mu}^2)}{({g_L^\mu}^2 + {g_R^\mu}^2)} \tag{38}$$

for which $A_{FB}^\mu = 3/4 A_\mu A_e$. We can define a similar A_f for any fermion f for which we can measure $\cos\theta$. In practice, this is all three charged leptons, e, μ, and τ, and the heavy quarks b and c (whose decays into leptons tell us whether we have a heavy quark or a heavy anti-quark[c] experiencing the decay. Obviously the top quark does not arise from Z decays, but we can use the same technique to measure a forward-backward asymmetry for it at Fermilab.

Homework: Derive $\overline{|\mathcal{M}|^2(e^+e^- \to Z \to f\bar{f})}$ for an arbitrary fermion f. Derive R_f and A_{FB}^f, and check your predictions for R_b and A_{FB}^b against their measured values.[4]

[c]Nonetheless, it is a subtle determination because meson-anti-meson mixing confuses things.

The Dark Secrets of the Terascale Downloaded from www.worldscientific.com by MONASH UNIVERSITY on 04/16/16. For personal use only.

5. $e^+e^- \to$ Hadrons

We have already seen the basics of $e^+e^- \to$ hadrons. At lowest order in perturbation theory, we can compute the rate into $q\bar{q}$ pairs, and sum over all of the quarks accessible at the energy of interest. In practice, we should still worry about a few details:

(1) Because the QCD coupling strength g_S is not very small, we should worry about the possibility that there could be a reasonably large chance to radiate additional quarks or gluons which will appear in our description of the final state.
(2) Quarks and gluons are not asymptotic states. Because of confinement, they are confined into colorless hadrons which are what actually interact with particle detectors.

The Dark Secrets of the Terascale Downloaded from www.worldscientific.com by MONASH UNIVERSITY on 04/16/16. For personal use only.

5.1. *Hadronization*

Let's discuss the second issue first, even though it is somewhat later in our picture of how a given event evolves from the initial annihilation to being detected. We have perfect evidence that quarks and gluons are always confined at large distances into hadrons. However, because this involves QCD at very low scales, the coupling is large and we can't use perturbation theory to understand it quantitatively. We can get some information from nonperturbative numerical simulations (such as lattice QCD), but even so, the state of the art is far away from being able to describe very complicated configurations of partons, such as occur in high energy collider reactions.

As a result, we have no first principles description of hadronization. To turn a set of models into a set of hadrons, we have to rely on models (popular computer codes such as `PYTHIA`[8] or `HERWIG`[9] contain different models, and it is worthwhile to remember that while all of them are reasonable, none of them are really absolutely correct). To discuss a definite picture, I will consider a "string"-like model, similar to (but not really the same as) the one used by `PYTHIA`.

First consider a $q\bar{q}$ pair, as shown in Figure 7a. Because of confinement, as they are produced and move away from one another (assuming they have some kinetic energy when created), a flux tube of gluon field stretches between them and tries to confine them. While we don't know much about this process, we can guess that the characteristics of the flux tube are determined by the scale of nonperturbative QCD, $\Lambda \sim 300$ MeV. In particular, up to order one numbers we can expect that the transverse sides of the tube are of order $\sim 1/\Lambda$ and the energy density inside the tube is Λ^4. Thus, the

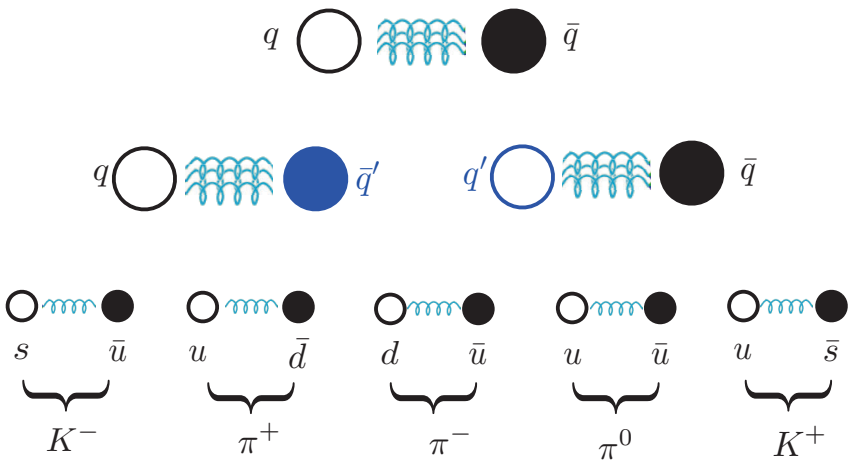

Fig. 7. Schematic picture for hadronization.

total energy contained in the string is:

$$E \sim \Lambda^2 L \tag{39}$$

where L is the string length, or in other words, the distance between the q and the $\bar{q}$.

As the quarks move apart, the string stretches, converting the kinetic energy into the energy of the flux tube. This can continue either until the quarks run out of kinetic energy, or there is enough energy stored in the flux of glue to create a $q'\bar{q}'$ pair. I write these as q' to emphasize that these could be differently flavored quarks than the ones I started with. In practice $m_d \sim m_u$ and m_s (and even in most cases m_c and m_b) are very small compared with the typical energies we encounter at modern colliders. After the creating the new pair of quarks, the string "snaps" into two strings, neither of which see any large color charge from the other, and so continue to evolve independently from one another (Figure 7b). Provided the quarks at its endpoint still have enough kinetic energy, each string will continue to grow, and continue to snap into pairs of light quarks when it can. Ultimately, this process will end when every quark has kinetic energy of order $\sim \Lambda$. At this point, the strings stop growing and we can identify the resulting hadrons by identifying each string with a meson.[d] An (overly

[d]Realistic models will also produce baryons, but this is beyond the scope of our cartoon discussion.

The Dark Secrets of the Terascale Downloaded from www.worldscientific.com by MONASH UNIVERSITY on 04/16/16. For personal use only.

simplified) example starting from the initial production of a pair of energetic strange quarks is shown in Figure 7c.

In practice the probability for the string to snap into a given flavored pair of quark and anti-quark and the probability for given final string whose end-points correspond to a comibation of one flavor and one anti-flavor to turn into a particular hadron are all described by parameters in the model which can be tuned to match data. Experience has shown that a certain amount of retuning of these parameters will need to be done at each new collider or center-of-mass energy to keep the predictions reasonably accurate.

The Dark Secrets of the Terascale Downloaded from www.worldscientific.com by MONASH UNIVERSITY on 04/16/16. For personal use only.

Moral: We don't *quantitatively* understand hadronization. If you are designing a measurement which depends very sensitively on the details of how it happens, you should treat whatever model you are using with deep suspicion. The differences between competing hadronization models may be large, and the spread in results they give may not capture the extent of the uncertainties in the model's predictions.

5.2. *Extra Radiation: The Parton Shower*

Now let's approach the second issue, the possibility of extra radiation. We know that in perturbation theory, the lowest order production of hadrons starts with $e^+e^- \to q\bar{q}$. The first possibility for radiation is from the process,

$$e^+e^- \to q\bar{q} + g \tag{40}$$

(see Figure 8) which is $\mathcal{O}(\alpha_S)$ compared to the leading rate. If we are working at high energies, say $s \simeq M_Z^2$, $\alpha_S \sim 0.1$, which is big enough that we need to be careful, but small enough that we can hope that perturbation theory can teach us something about how it works. The matrix element for producing $q\bar{q}$ along with a gluon of color index a is,

$$\begin{aligned} -i\mathcal{M} = &\left[\bar{u}_f i g_S \lambda^a \not{\epsilon}_g i \frac{(\not{p}_q + \not{p}_g + m_q)}{(p_q + p_g)^2 - m_q^2}\gamma^\mu v_{\bar{q}}\right] \\ &+ \left[\bar{u}_q \gamma^\mu i \frac{(-\not{p}_{\bar{q}} - \not{p}_g + m_q)}{(p_{\bar{q}} + p_g)^2 - m_q^2} i g_S \lambda^a \not{\epsilon}_g v_{\bar{q}}\right] \end{aligned} \tag{41}$$

where λ^a is the Gell-Mann color matrix, ϵ_g^μ is the gluon polarization vector, and g_S is the strong coupling constant. I have included the gamma matrix γ^μ alluding to the possibility that our original $q\bar{q}$ pair were the result of virtual photon exchange, but it should become clear very soon that the actual production mechanism of the $q\bar{q}$ is not important, and our results

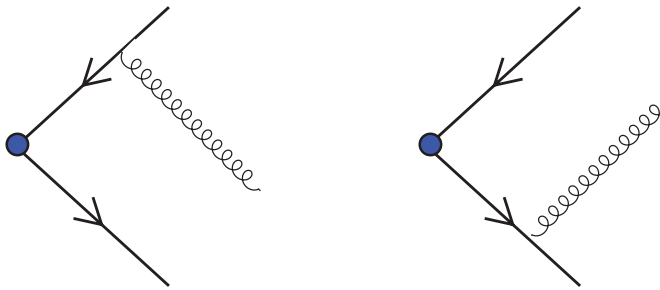

Fig. 8. Feynman diagrams for $q\bar{q}g$ production. The blue circles represent any interaction which can produce a $q\bar{q}$ pair; in the explicit calculations I will assume that this was a vertex for an incoming γ^*.

The Dark Secrets of the Terascale Downloaded from www.worldscientific.com by MONASH UNIVERSITY on 04/16/16. For personal use only.

will hold equally well for production through exchange of a Z boson or any other particle (not necessarily s-channel or even a vector).

Let's focus on the graph where the gluon is radiated from the quark. We have kept the quark mass, despite the fact that we are interested in high energy production where $E \gg m_q$. In general, we will go ahead and ignore m_q, but it is helpful to remember where it appears as we proceed with the discussion below. The propagator can be expanded in terms of the final state gluon energy E_g, the final state quark energy E_q, and the angle in between their spatial momenta θ_{qg}:

$$(p_g + p_q)^2 \simeq 2p_g \cdot p_q = 2E_g E_q \left(1 - \cos\theta_{qg}\right) \tag{42}$$

we can see that there are two problem regions where the graph becomes large:

$$E_g \to 0 : \text{soft region}$$
$$\cos\theta_{qg} \to 1 : \text{collinear region}$$

For both regions, the propagator denominator seems to vanish (at least for $m_q \to 0$), and the amplitude becomes large. These facts already motivate the idea that there is a large probability for there to be extra soft or collinear radiation present. However, we can work at a more quantitative level to see how this works explicitly.

As we proceed, it will be useful to switch notation slightly. Let's call by p_q the *original* quark 4-momentum, before it splits into the *final* quark carrying momentum p_f and the final gluon momentum p_g. We'll choose to align our $\hat{z}$-axis along the direction of the original quark 3-momentum and the $\hat{x}$-axis along the direction of the emitted gluon momentum which is

transverse to the $\hat{z}$-axis. In order to split into a real gluon and final quark, that means the original quark must be slightly off-shell. So we can write:

$$\begin{aligned} p_q &= (E,\ \ 0,\ \ 0,\ \ p) \\ p_g &= \left(zE,\ zp_T,\ 0, z\sqrt{E^2 - p_T^2}\right) \\ p_f &= \left((1-z)E,\ \ -zp_T,\ 0, \sqrt{(1-z)^2E^2 - z^2p_T^2}\right) \end{aligned} \tag{43}$$

where z is a real number between zero and one which measures the fraction of energy from the original quark carried away by the gluon, and the $\hat{z}$ components of p_f and p_g are determined by the fact that they are final state (approximately) massless particles. In this language, the soft region is $z \to 0$ and the collinear region is $p_T \to 0$.

First, let's discuss the soft region. A gluon with no energy essentially does not exist. It cannot escape from the quark nearby to it, and is really nothing more than a label keeping track of color. It will get bound inside whatever hadron captures the nearby quark. Thus, from the point of view of observation, it is not distinguishable from just having a $q\bar{q}$ final state. Thus, to consistently speak about this order of perturbation theory, we should include the one-loop diagram with a gluon attached to the quarks (Figure 9). This gluon is completely virtual and the graph's interference with the leading order production is the same order (LO $\times\ \alpha_S$) as the emission diagram squared. The Kinoshita-Lee-Naumberg (KLN) theorem guarantees that the soft singularity in the one-loop and the emission diagrams will cancel at any order in perturbation theory. Thus, once we properly sum the one-loop and the soft region of the real emission diagrams appropriately, we need not worry.

The collinear region is defined by small p_T. If we expand the quark propagator momentum p_q as a series in p_T/E, we find

$$p_q^2 \simeq \frac{z\ p_T^2}{(1-z)} \tag{44}$$

In this limit, the matrix element for our first Feynman diagram becomes,

$$\mathcal{M}_1 \to [\bar{u}_f\ ig_S\lambda^a\ \not{\epsilon}_g i(\not{p}_q + m_q)\gamma^\mu v_{\bar{q}}] \times \frac{(1-z)}{z(p_T^2 + m_q^2)}\ , \tag{45}$$

where I have reintroduced m_q^2 just to act as a regulator for the collinear divergence, and I am being a little careless with the numbers that multiply it for that reason. Since for $p_T \to 0$, p_q goes on-shell, we can replace it with

The Dark Secrets of the Terascale Downloaded from www.worldscientific.com by MONASH UNIVERSITY on 04/16/16. For personal use only.

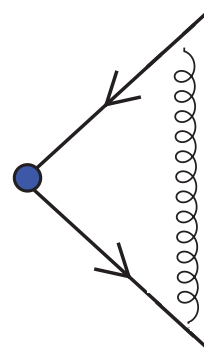

Fig. 9. Virtual gluon exchange.

a sum over polarizations of the corresponding on-shell spinor[e]:

$$\not{p}_q + m_q \to \sum_{(s)} u_q^{(s)} \bar{u}_q^{(s)} \ . \tag{46}$$

and the matrix element separates into two factors:

$$\mathcal{M} \to \sum_{(s)} -ig_S \left[\bar{u}_f \lambda^a \not{\epsilon}_g u_q^{(s)}\right] \times \frac{(1-z)}{z(p_T^2 + m_q^2)} \times \left[\bar{u}_q^{(s)} \gamma^\mu v_{\bar{q}}\right] \tag{47}$$

where the first factor describes the emission of the gluon and the second factor is just the LO matrix element to produce the original $q\bar{q}$ pair. It should be pretty clear from the derivation here that this *factorization* of the amplitude occurs independently of how the original $q\bar{q}$ are produced: a different production process will just result in the appropriate matrix element appearing as the rightmost factor in the expression. We say that in the collinear limit, the amplitude factorizes into the leading order production matrix element times a factor that is always the same for any collinear gluon emitted from a quark, regardless of where that original quark actually came from. It should also be clear that we can repeat this argument for the second diagram where the anti-quark emits the gluon, and we will find the same kind of factorization. In fact, with some thought you should be able to convince yourself that the same kind of reasoning can be applied to graphs with *multiple* collinear gluons emitted. As long as they are all collinear, each emission produces the leading $e^+e^- \to q\bar{q}$ matrix element

[e]I learned this trick from.[3] It makes this derivation MUCH clearer than the alternative I had planned to use.

The Dark Secrets of the Terascale Downloaded from www.worldscientific.com by MONASH UNIVERSITY on 04/16/16. For personal use only.

times a product of factorized sub-amplitudes which describe the splitting of a quark into a quark + a collinear gluon as a function of its energy fraction and relative p_T.

For our specific process, we have found,

$$\mathcal{M}(e^+e^- \to q\bar{q}g_{\text{collinear}}) = \mathcal{M}(e^+e^- \to q\bar{q}) \times \frac{(1-z)}{z(p_T^2 + m_q^2)} \times \mathcal{M}(q \to qg_{\text{collinear}}) \tag{48}$$

where $\mathcal{M}(q \to qg_{\text{collinear}})$ is a function of z, the fraction of energy that the gluon takes from its parent quark, and depends on the relative p_T between the parent quark and radiated gluon as $1/p_T^2$. To turn this into a cross section, we square the matrix element, and integrate over the final state momenta. Let's introduce some short-hand:

$$d\Phi_3(p_f, p_g, p_{\bar{q}}) \equiv \frac{d^3p_f}{2E_f(2\pi)^3} \frac{d^3p_g}{2E_g(2\pi)^3} \frac{d^3p_{\bar{q}}}{2E_{\bar{q}}(2\pi)^3} \times (2\pi)^4\delta^4(p_a + p_b - p_f - p_g - p_{\bar{q}}) \tag{49}$$

and now we can write the cross section by splitting the integration between the collinear and noncollinear regions as:

$$\begin{aligned}
\sigma(e^+e^- \to q\bar{q}g) &= \int d\Phi_3(p_f, p_g, p_{\bar{q}}) \quad \overline{|\mathcal{M}(e^+e^- \to q\bar{q}g)|^2} \\
&= \int_{p_T^2 < \mu^2} d\Phi_3(p_f, p_g, p_{\bar{q}}) \quad \overline{|\mathcal{M}(e^+e^- \to q\bar{q})|^2} \\
&\qquad \times \frac{(1-z)^2}{z^2(p_T^2 + m_q^2)} \times \frac{\overline{|\mathcal{M}(q \to qg_{\text{collinear}})|^2}}{p_T^2} \\
&\quad + \int_{p_T^2 > \mu^2} d\Phi_3(p_f, p_g, p_{\bar{q}}) \quad \overline{|\mathcal{M}(e^+e^- \to q\bar{q}g_{\text{nc}})|^2}
\end{aligned}$$

where we have introduced a scale μ which defines what we consider to be collinear or noncollinear, and we organized the $(p_T^2 + m_q^2)^2$ denominator with one factor together with the matrix element for collinear splitting because it will eventually turn out to be proportional to p_T^2, and so this factor is actually independent of p_T. Note also that I should have also separated out the part where the p_T between the gluon and $\bar{q}$ is less than μ, but it is easy to follow our derivation and reconstruct these terms, so I will leave it for you to do.

The Dark Secrets of the Terascale Downloaded from www.worldscientific.com by MONASH UNIVERSITY on 04/16/16. For personal use only.

The Dark Secrets of the Terascale Downloaded from www.worldscientific.com by MONASH UNIVERSITY on 04/16/16. For personal use only.

In principle we can choose any value for μ that we find convenient, but in practice we should choose μ small enough that the approximations made in the first term's matrix elements are valid. The second (noncollinear or "nc") term contains no problematic propagators, and so we can expect that it will be naturally of order $\alpha_S \sim 0.1$ times the LO diagram. In other words, it is a small correction to the LO rate, and does not qualitatively change the picture, but instead is a modest quantitative correction to it.

Now let's finish up with the collinear term. We can rewrite the phase space integrals as:

$$d\Phi_3(p_f, p_g, p_{\bar{q}}) = d\Phi_2(P; p_q, p_{\bar{q}})\; d\Phi_2(q; p_f, p_g)\;\; \frac{dp_q^2}{2\pi} \tag{50}$$

where we used our phase space recursion decomposition, Eq. (16). The region with small p_T is also the region with $p_q^2 \simeq 0$ (see Eq. (44)), so we can convert the integration over p_q^2 into an integration over p_T^2:

$$dp_q^2 = \frac{z}{1-z} dp_T^2 \; . \tag{51}$$

Note also that for small p_q^2, inside the collinear term we have $\overline{|\mathcal{M}(e^+e^- \to q\bar{q})|^2} d\Phi_2(P; p_q, p_{\bar{q}})$, which integrates

where in the second equality of the last line, I went ahead and did the integral over $d\phi$. Combining this with our factorized matrix elements, and doing the integrals over $d\Pi_q \; d\Pi_{\bar{q}} \; dp_T^2$, we find:

$$\sigma(e^+e^- \to q\bar{q}g_{\rm collinear}) = \int dz \; \frac{1}{16\pi^2} \; \left[\frac{(1-z)^4}{z^3} \frac{\overline{|\mathcal{M}(q \to qg_{\rm collinear})|^2}}{p_T^2} \right] \times \log\left(\frac{\mu^2}{m_q^2}\right) \sigma(e^+e^- \to q\bar{q}) \tag{52}$$

We can work out the matrix element squared for gluon emission as a function of z. It's customary to extract out the g_S^2 and the sum/average over colors from it, and write,

$$\sigma(e^+e^- \to q\bar{q}g_{\rm collinear}) = \sigma(e^+e^- \to q\bar{q}) \times \; \frac{\alpha_S}{2\pi} \; \frac{4}{3} \; \log\frac{\mu^2}{m_q^2} \; \int dz \; P_{q\to g}(z) \tag{53}$$

where

$$P_{q\to g}(z) = \frac{1+(1-z)^2}{z} \tag{54}$$

is called the splitting function.

Homework: Derive the splitting function $P_{q\to g}(z)$ by squaring the matrix element $\mathcal{M}(q \to qg_{\text{collinear}})$ and summing and averaging it appropriately over spin and color.

These results make it clear why jets of partons ultimately emerge from production of a single hard parton. A collinear splitting produces a factor[f] of $\alpha_S \times \log(\mu^2/m_q^2)$. If $\mu >> m_q$ (and I'll say more about this below), the rate for producing the $q\bar{q}$ pair together with a collinear gluon can be greater than the rate of production of a $q\bar{q}$ pair by itself, because the log can compensate for α_S. This is an indication that usual perturbation theory is sick, and can't be trusted. However, the fact that this badly behaved region also leads to factorization means that if I am clever, I can "re-sum" those parts of phase space to all orders, because I can easily write down the expression to any order I want, given the leading order matrix elements and the splitting functions. The showering Monte Carlo programs use the factorization theorem to numerically estimate how likely it is to get a given configuration of collinear partons. Since the parton shower is derived from perturbative QCD, we can trust it to describe the collinear region pretty accurately. Where we should not trust it is to correctly describe additional radiation at wide angles – we need the exact matrix elements to describe those kinematics.

One should keep firmly in mind that the scale μ is something we invented to conveniently cut up the phase space of the gluon. The original problem knew nothing of such a scale, and just as in the case of renormalization, we can sometimes use this fact to our advantage. Since we were able to compute the dependence of the collinear piece of term and found it to go like $\log \mu^2$, we know that this explicit dependence must be cancelled by the noncollinear piece, which must also contain an implicit log dependence on μ. Since μ is dimensionful and the argument of a log should be dimensionless, something from the high energy process needs to appear to cancel the dimensions of μ in the argument of the log. In the case of $e^+e^- \to q\bar{q}g$, the only dimensionful quantities are the Lorentz invariants which describe the initial state beam momenta and the final state parton momenta. For this process, all of these are of the order of the Mandelstam s variable. So I should

[f]I should mention again at this point that because of confinement, m_q is not particularly meaningful as a kinematic quantity. Any light quark of low enough energy for me to "notice that it has a mass", is really confined in a hadron. So it would be more appropriate to replace m_q by Λ, the QCD scale, in the logarithm. This choice also more easily allows us to hand off a "showered" simulation of an event to a hadronization model.

The Dark Secrets of the Terascale Downloaded from www.worldscientific.com by MONASH UNIVERSITY on 04/16/16. For personal use only.

choose $\mu^2 \sim s$ in order to keep perturbation theory in the noncollinear terms under control. In practice, if someone has already done the complete higher order calculation, I know exactly which invariants appear together with μ in the logs, and I can make a more informed decision about how to choose it.

A few comments to wrap up this discussion: First of all, notice that the discussion of collinear emission made to reference to confinement. In fact, for high enough energy processes involving low enough mass fermions, we are guaranteed to get into a regime where perturbation theory breaks down and needs to be improved in the way we have discussed. This is even true for QED at energies where $\log(s/m_e^2) \sim 1/\alpha$. The reason for jets of collinear particles is not really because the coupling is strong, but instead because quarks and gluons are (nearly) massless; the strength of the coupling determines at which energy the phenomenon emerges, not the fact that it occurs.

The Dark Secrets of the Terascale Downloaded from www.worldscientific.com by MONASH UNIVERSITY on 04/16/16. For personal use only.

5.3. *Jets*

In practice, the parton shower takes a primary hard parton and turns it into a whole collection of softer partons (and eventually via the hadronization model, hadrons) moving in roughly the same direction. These spread out and hit slightly different parts of the detectors, resulting in an experimental problem in which we need to correctly group the individual detector cells together to reconstruct the energy of the original parton. In practice, this can only ever be a statistical game, in which one designs an algorithm for clustering hadrons together which works most of the time. The code `FastJet`[10] provides some tools one can use to implement many of the popular jet algorithms with relative ease.

For simple purposes, it is not completely crazy to work at the level of the hard partons and treat the initially produced quarks and gluons as cones of energy centered on the parent parton momentum. More detailed questions depend on correctly simulating the parton shower and choosing a jet algorithm, but if your question doesn't require deeply rigorous treatment, this is not a bad place to start. A rule of thumb is: for jet energies on the order of hundreds of GeV, a typical high energy particle detector will be able to detect its presence with very high efficiency, and the complications of showering and jet clustering will smear the reconstructed energy relative to the parent parton and spread out the jet constituents into roughly a cone centered on the parent parton.

6. Hadron Colliders

Hadron colliders are currently the tools which provide the most energetic reactions. As of a few days before this writing, the LHC experiments have collected ~ 1 fb^{-1} and the next year will find them well-poised to make significant statements about the Higgs and new physics.

The really new feature of high energy hadronic reactions is the fact that any given reaction involves partons carrying a fraction of their parent hadron's energy. As a result, for any given event we do not control the initial state at the parton level and instead see a statistical distribution of combinations of quarks and/or gluons carrying a distribution of initial energies.

The Dark Secrets of the Terascale Downloaded from www.worldscientific.com by MONASH UNIVERSITY on 04/16/16. For personal use only.

6.1. *Parton Distribution Functions*

The initial mapping from a parent hadron to a child parton carrying a fraction x of its parent's energy is described by the parton distribution functions (PDFs) typically denoted $f_{p/H}(x, \mu)$, where p labels the parton participating in the large energy scattering, H is the type of parent hadron, and x the fraction of the hadron's energy carried by the parton.[g] There is a schematic picture in Figure 10. A factorization theorem similar to the one derived above allows us to define universal PDFs for all high energy processes. These theorems are really the key to our understanding of hadronic collisions: we have a limited set of functions which we can measure carefully at one experiment, and the same functions allow us to make predictions at future experiments.

In principle, describing the matrix elements for the overlap of the initial hadron state with the intermediate "initial" partons is just as nonperturbative and incalculable as the hadronization models described above. The difference is that because we have isolated the nonperturbative input into a relatively small number of functions for which we have a wealth of precise data, these functions are actually pretty well known. The initial partons can also radiate quarks and gluons, and have the same collinear singularities we saw in the final state of $e^+e^- \to q\bar{q}g$ when the internal parton goes on the mass shell. Once again, a factorization scale μ describes the division of phase space into collinear (enhanced) and noncollinear (perturbative correction) regimes. Thus, when one measures the PDFs, one needs to choose a scale in the perturbative calculation, and the PDFs become functions

[g]In fixed target collisions, x should be interpreted as the fraction of the light cone momentum p_+.

The Dark Secrets of the Terascale Downloaded from www.worldscientific.com by MONASH UNIVERSITY on 04/16/16. For personal use only.

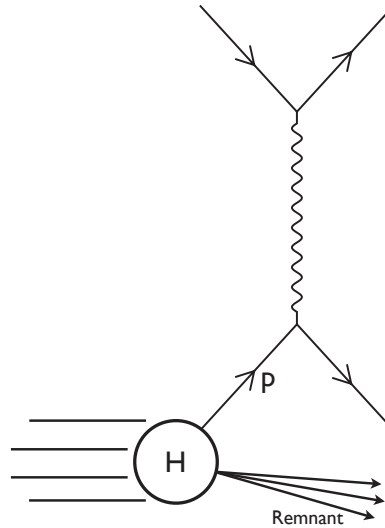

Fig. 10. Schematic picture of a hadron undergoing high energy scattering through one of its constituent partons.

of this scale choice. However, since we understand the dependence on this scale in terms of the splitting functions, we know how to use perturbation theory to evolve the PDFs at one scale into any other scale at which α_S is perturbative. So in principle, if we had a perfect measurement of the all of the PDFs at one scale, we would know them at any other scale. In practice, the PDFs are global fits to data collected from observables characterized by a variety of scales.

Much of the data driving the fits to the PDFs was collected at the HERA collider, an $e^{\pm}p$ machine operating at a center of momentum energy of 318 GeV. The basic process is depicted in Figure 10. We can relate the cross section for proton-electron scattering (which for low momentum transfer can be approximated as pure photon exchange) at lowest order in perturbation theory as,

$$\sigma\left(pe^- \to e^- + \text{jet}\right) = \sum_q \int \frac{dx}{x} f_{q/p}(x,\mu)\ \sigma\left(q(xE_p)e^- \to e^- + \text{jet}\right)\ . \quad (55)$$

By measuring the out-going electron kinematics (and knowing its incoming energy), one can reconstruct the momentum transfer (which provides an appropriate choice for μ) and the x of a particular collision. At higher orders in perturbation theory, one also becomes sensitive to the gluon distribution.

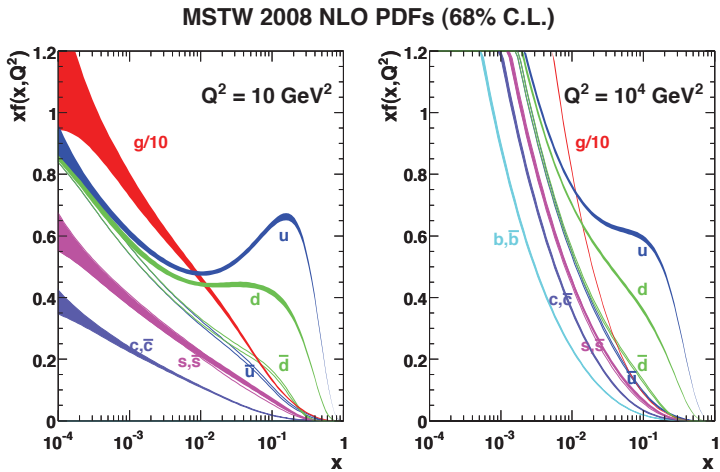

Fig. 11. MSTW parton distribution functions plotted as $xf(x)$ versus x at two different energy scales. The width of each band reflects the uncertainty at that point. From.[11]

You can find global fits of the set of $f(x)$ to very large sets of data available in easy-to-use packages such as MSTW[11] or CTEQ.[12] In Figure 11, we show the MSTW PDFs, plotted as $xf(x)$ for two choices of factorization scale as a function of x. The width of each band represents a measure of the uncertainty in that particular function. A few obvious trends are that all of the PDFs fall quickly as $x \to 1$, and at very large momentum fraction x the valence u and d quarks dominate. At smaller x, the gluon (which is divided by 10 in the figure) is the single largest contributor. One can obtain the PDFs for anti-protons by replacing the valence quarks $u \leftrightarrow \bar{u}$ and $d \leftrightarrow \bar{d}$ in the proton PDFs. The PDFs for neutrons are obtained by replacing $u \leftrightarrow d$ and $\bar{u} \leftrightarrow \bar{d}$.

The fact that high energy collisions actually involve partons carrying a fraction of the parent hadron complicates the analysis of the reactions somewhat. Consider the collision of p and $\bar{p}$ (such as at Fermilab) to produce a lepton pair:

$$\begin{aligned}\sigma\left(p\bar{p} \to e^+e^-\right) &= \sum_q \int \frac{dx_1}{x_1}\frac{dx_2}{x_2}\left\{f_{q/p}(x_1)f_{\bar{q}/\bar{p}}(x_2)\ \ \sigma\left(q(x_1E_p)\bar{q}(x_2E_{\bar{p}}) \to e^+e^-\right)\right. \\ &\left. +\ f_{\bar{q}/p}(x_1)f_{q/\bar{p}}(x_2)\ \ \sigma\left(q(x_2E_{\bar{p}})\bar{q}(x_1E_p) \to e^+e^-\right)\right\} \qquad (56)\end{aligned}$$

The Dark Secrets of the Terascale Downloaded from www.worldscientific.com by MONASH UNIVERSITY on 04/16/16. For personal use only.

The Dark Secrets of the Terascale Downloaded from www.worldscientific.com
by MONASH UNIVERSITY on 04/16/16. For personal use only.

where I have suppressed the PDF dependence on μ just to keep the expression more compact and explicitly used the fact that in the Standard Model, only quarks and anti-quarks of the same flavor can annihilate at tree level into leptons. The two terms keep track of the fact that it is possible to get the quark out of the proton (and the $\bar{q}$ from the $\bar{p}$) or vice-versa (though looking at Figure 11 makes it clear that it is much more likely that the former will happen than the latter). Note that $\sigma(q\bar{q} \to e^+e^-)$ is the time-reversal of same process we discussed before. Since under time reversal, $s \to s$ and $t \to t$, we already know just about everything there is to worry about here.

Any given event will correspond to initial parton kinematics described by the values of x_1 and x_2. In practice, nothing we can measure in the hadronic reaction tells us what these values are, or even whether x_1 describes the quark and x_2 the anti-quark, or vice-versa. Thus, even if the lab frame is the center of momentum frame of the hadrons, for any given event the hard part of the scattering will have a net boost along the beam direction proportional to $x_1 - x_2$, and we need to use measurements of the final state to learn about the center of momentum collision energy for any particular event. In practice, this makes searches involving invisible particles like neutrinos (or dark matter) much more challenging at hadron colliders than at e^+e^- machines.

6.1.1. *Cross sections at Hadron Colliders*

We now describe some qualitative features of cross sections physical processes at Hadron Colliders. The main determining factors are

- *Energy threshold*
  Every physical process has a characteristic energy threshold. This can be either the masses of the particles being produced, or the kinematical cuts being imposed. Since the PDFs are steeply falling functions of momentum fraction x, most of the events of a physical process will occur close to the threshold, $E_{\rm collision} = \sqrt{x_1 x_2} E^{pp}_{\rm cm} \sim E_{\rm threshold}$. For the same reason, the cross sections will decrease sharply with the increase of the energy threshold. An important example is the production cross section of new physics particle(s) with mass M, which falls very fast $\sigma_{\rm np} \sim 1/M^{6-8}$. This is the most import limitation on the reach of new physics at hadron colliders.

- *Initial state*
  PDFs for different partons can be very different. From the right panel of Fig. 11, we see that gluon dominates for x less than about 10^{-2}, while all

the (anti)quarks are similar (with the possible exception of $b\bar{b}$). Therefore, in this regime, any process which can come from gg initial state, such as the pair production of colored particles, will have the largest cross section. Processes starting with $q(\bar{q})g$ will be down by about $10-100$, from f_q/f_g. For the same reason, processes starting with $qq(\bar{q})$ will be further suppressed. For larger momentum fractions, $x > 10^{-2}$, the u and d (the so called valence quarks) start to dominate the PDFs. Therefore, any process starting from valence quark(s) with be enhanced accordingly. This is a good place to mention one of the key differences between a pp collider and a $p\bar{p}$ collider. For the anti-proton, $\bar{u}$ and $\bar{d}$ are the valence quarks. Therefore, for the same (and large) x, $q\bar{q}$ initiated processes will have a larger cross section at a $p\bar{p}$ collider than at a pp collider.

There are many physical processes can start with several different initial states. For example, $t\bar{t}$ production in the SM can start with both gg and $q\bar{q}$ initial states. Obviously, processes which can originate from more initial states will accordingly have larger cross sections.

- *Final state multiplicity*
  Different physical processes can have different number of particles in the final state. From the expression of cross section, there is a phase space factor of $d^3p_f/[2E_f(2\pi)^3]$ for each final state particle. After integrating over phase space, this leads to roughly a 10^{-2} suppression for each final state particle. Therefore, for example, $pp \to t\bar{t}h$ process has a much smaller production cross section than the process with one less final state particle, $pp \to t\bar{t}$.

- *Couplings*
  Obviously, the strength of the interaction mediating the scattering process enters directly into the size of the cross section. In any Feynman diagram, each vertex contains a coupling, which leads to a factor of (coupling)^2 in the cross section.[h] We typically work in the regime of the theory with a perturbative expansion in powers of small coupling constants. Therefore, more "complicated" Feynman diagrams are further suppressed. For example, in addition to the phase space suppression discussed above, processes with one additional final state particle will be further suppressed by an additional factor of (weak coupling)^2.

[h]There can be important interference effects, which are proportional linearly to the coupling constant.

The Dark Secrets of the Terascale Downloaded from www.worldscientific.com by MONASH UNIVERSITY on 04/16/16. For personal use only.

- *Singularities*
  Loosely speaking, what we have discussed so far applies to the cases in which $|\mathcal{M}|^2$ of the scattering process are smooth functions of kinematical variables. There are important exceptions. One important class of this kind consists of soft and collinear singularities discussed earlier in the lecture. Another important example is resonant production. Consider, for example, the process $pp \to \mu^+\mu^-$ in the SM. In general, we should (correctly) regard this as a $2 \to 2$ process. However, the scattering amplitude has a pole at $\hat{s} = x_1 x_2 (E_{\rm cm}^{pp})^2 = m_Z^2$. Therefore, in this regime, we should approximately regard this as a $2 \to 1$ process $pp \to Z$, followed by a decay process $Z \to \mu^+\mu^-$. More details of this process will be discussed in Section 6.3.

The Dark Secrets of the Terascale Downloaded from www.worldscientific.com by MONASH UNIVERSITY on 04/16/16. For personal use only.

6.2. *Cartoon of a Collider Detector*

Before discussing some particular observables, it is useful to develop a mental picture of what a collider detector looks like and how it measures particles. While in principle, there is a very sophisticated simulation modeling any particular detector, in practice these simulations are not available to theorists, and we should be able to get roughly correct ideas for what can or cannot be measured from a simple picture.

To begin with, the angle in a hadron collider is usually expressed in terms of the pseudorapidity,

$$\eta \equiv -\log\left[\tan\left(\frac{\theta}{2}\right)\right] \ . \tag{57}$$

$\eta = 0$ is the direction perpendicular to the beam axis, and increasing η in the positive sense moves (in the logarithmic steps) toward the positive $\hat{z}$ axis. For massless particles, η is equivalent to the rapidity,

$$y \equiv \frac{1}{2}\log\left[\frac{E + p_z}{E - p_z}\right] \ . \tag{58}$$

In practice, we are often sloppy when speaking, and will say "rapidity" even when we technically mean pseudo-rapidity. For massless particles, this confusion doesn't really matter, but it is worth emphasizing that for massive particles they are not the same. In particular, particle detectors themselves really determine η.

The nice thing about these variables is that for boosts along the beam axis, y transforms additively. If we do a $\hat{z}$-boost characterized by boost

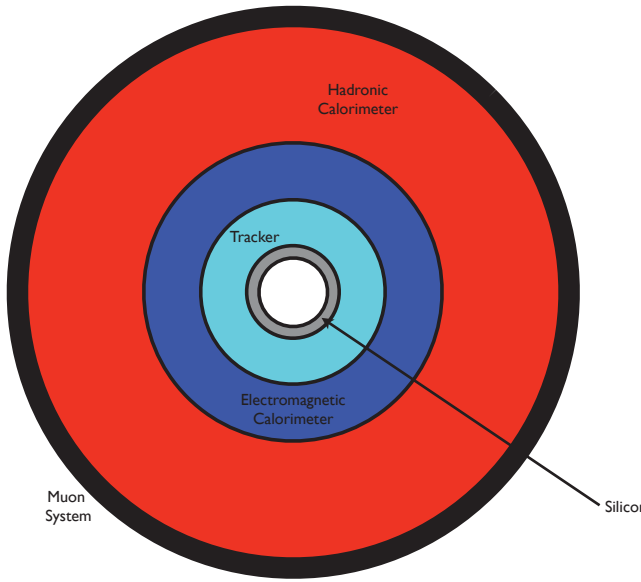

Fig. 12. A cartoon cross section of a collider detector.

parameter β, the transformed rapidity is,

$$y^{\text{boosted}} = y^{\text{original}} + \frac{1}{2}\log\left(\frac{1+\beta}{1-\beta}\right) \ . \tag{59}$$

The connection between the lab frame and the parton center of momentum frame is given by,

$$\beta = \frac{x_1 - x_2}{x_1 + x_2} \ . \tag{60}$$

Now let's look at a cross section of a cartoon collider detector. In Figure 12, which shows a cross sectional slice of the detector looking along the beam line. The detector is approximately cylindrically symmetric, and has a series of concentric elements centered on the beam axis designed to catch different types of particles. Moving outward from the beam, the elements typically include:

- A Silicon tracker with a size on the order of cm, designed to track charged particles very close to the interaction point. This precise tracker aims to accurately reconstruct the tracks close enough to the interaction point so as to be able to detect decays of heavy quarks separated from the primary interaction point.

The Dark Secrets of the Terascale Downloaded from www.worldscientific.com
by MONASH UNIVERSITY on 04/16/16. For personal use only.

- A larger and less precise tracker on the order of ~ 100 cm, which measures charged particle tracks (and through their bending in the magnetic field, their momenta).
- An electromagnetic (EM) calorimeter with a size on the order of $\sim$ m, designed to measure energies of photons and charged particles.
- A hadronic calorimeter of $\sim$ m scale size designed to measure the energy of hadrons.
- A muon system which is designed to identify and measure the energy of muons.

The Dark Secrets of the Terascale Downloaded from www.worldscientific.com by MONASH UNIVERSITY on 04/16/16. For personal use only.

These components work together to provide object identification:

- **Jets** appear as collections of large numbers of hadrons close together in a region of the detector. Since there are typically many constituents, some electrically charged and some neutral, a jet will typically have many tracks associated with it, along with some energy in the electromagnetic calorimeter and a large amount in the hadronic calorimeter. In addition, radiation and decay of the component hadrons may produce (typically low energy) photons, electrons, and/or muons inside the jet.
- **Bottom-jets** are jets initiated by a hard bottom quark. Since they contain a b quark, they will typically contain a b-flavored hadron, whose typical lifetime can be long enough that it travels a macroscopic distance before decaying. Since the decay is displaced from the primary interaction vertex, b-jets can be distinguished from ordinary jets by reconstructing the secondary vertex associated with the decay.
- **Photons** will typically deposit most of their energy in the electromagnetic calorimeter, but being electrically neutral, do not have a track associated with them.
- **Electrons** will typically lose their energy in the EM calorimeter, and do have a track associated with the energy deposition.
- **Muons** have a track, but do not lose much energy until they reach the muon system in the outer part of the detector.
- **Tau** leptons have hadronic decays (also producing neutrinos) which are sometimes reconstructed as jets with small sizes and numbers of particles, making them very challenging to identify.
- **Neutrinos** interact too weakly to be detected at all. Their presence can often be inferred through seeing an imbalance in the final state momenta of the visible particles.

If there are new kinds of charged or hadronic particles which live long enough to reach the detectors, they can usually be reconstructed through

the unusual way in which they lose kinetic energy as they traverse the detector elements.[13]

6.3. *Resonance Signals*

Now let's look at one of the classic signals of physics beyond the Standard Model: a resonance. The usual example of a new resonance is a new neutral gauge boson, or Z', which is something that often occurs in theories of physics beyond the Standard Model. For example, if nature realizes an $SO(10)$ GUT, breaking down to the MSSM involves an extra diagonal generator which can break at a much lower scale and produces a Z'. Similarly, left-right models have a neutral W_R, little Higgs theories have an extended gauge sector, and KK theories may have towers of SM gauge bosons, all of which contain objects which behave like some kind of Z'.

If a Z' couples to both quarks and leptons, it can contribute to the process $q\bar{q} \to e^+e^-$, in analogy with the SM Z boson exchange graph of Figure 2. Despite the fact that we don't know the initial state energies of the colliding partons, we can still easily look for this kind of new particle by constructing the invariant mass of the final state leptons, $M_{ee} \equiv \sqrt{(p_{e^+} + p_{e^-})^2}$. At tree level, this is actually just the square-root of the partonic Mandelstam s variable. Since there are also photon and Z boson exchange graphs, we expect to see the same kind of structure we saw in $e^+e^- \to$ hadrons, with an extra resonance at the position of $M_{Z'}$. The only qualitative difference is that the PDFs will cause the rate to fall off faster than the $1/s$ behavior we saw before, because they themselves fall with larger s. This behavior is illustrated in Figure 13. In practice, the experimentalists can fit the region at small s where the photon and SM Z boson dominate, and use it to calibrate their background models.

Discovering a Z' in this way would immediately give a measurement of its mass, as the position of the bump in M_{ee}, and an upper bound on its inclusive decay width, as the width of the Breit-Wigner. It will turn out to be a measurement of the width if the width is larger than the experimental resolution on M_{ee} close to $M_{Z'}$, and otherwise an upper bound. The height of the resonance above the SM background can be related to a sum of quark couplings weighted by PDFs times the branching ratio into e^+e^-.[14–17] If we can measure several decay modes, we can get ratios of $g_L^2 + g_R^2$ for as many different fermions as we can identify, in analogy to the R_f ratios that were useful to analyze the Z boson decays.[i]

[i]In practice, it is probably not convenient to normalize to the decays into hadrons here, because this channel will have a large SM background from QCD production of two jets.

The Dark Secrets of the Terascale Downloaded from www.worldscientific.com by MONASH UNIVERSITY on 04/16/16. For personal use only.

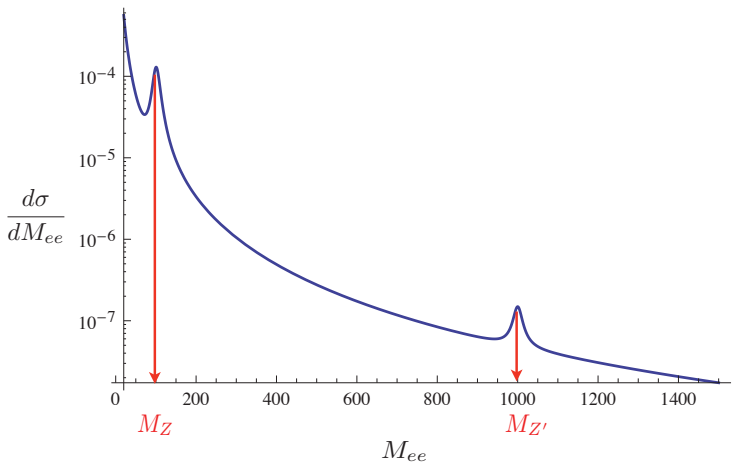

Fig. 13. Distribution of $d\sigma/dM_{ee}$ in the reaction $pp \to e^+e^-$, including the SM γ and Z contributions, along with a new Z' boson .

The remaining quantities we would like to measure are the analogues of the A_{FB}^f observables. At the LHC, this is a somewhat subtle point. Because we don't know which proton donates the quark and which the anti-quark, we cannot actually define the direction of the positive $\hat{z}$-axis. As a result, for any given event, we can't tell $\cos\theta$ from $-\cos\theta$, which means we don't know how to construct the observable that picks out the $g_L^2 - g_R^2$ dependence. However, it is possible to reconstruct something useful in a statistical sense. Since the valence quark PDFs are much larger than the anti-quarks or the sea quarks, we can expect that unless the Z' has strongly family-dependent couplings, most of its production will be through a mix of initial states containing $u\bar{u}$ and $d\bar{d}$. Since the valence quark PDFs have support out to larger values of parton x, for any given Z' event it is more likely that the net boost of the system will be in the direction that the incoming quark was traveling than the anti-quark. Thus, for each event I can choose the positive $\hat{z}$-axis along the direction of the net boost of the e^+e^- pair, and I will choose it correctly somewhat more often than incorrectly, and I can extract a meaningful A_{FB} measurement. Interested readers should consult the more sophisticated discussion which can be found in Ref.[18]

6.4. *Missing Energy Signals*

Our second example of a signal of physics beyond the Standard Model is missing transverse momentum. We typically refer to such signals as

The Dark Secrets of the Terascale Downloaded from www.worldscientific.com by MONASH UNIVERSITY on 04/16/16. For personal use only.

The Dark Secrets of the Terascale Downloaded from www.worldscientific.com by MONASH UNIVERSITY on 04/16/16. For personal use only.

missing energy, because in practice an important part of how we construct the momentum of visible particles is through measuring their energies in the calorimeters and using the on-shell relation together with directional measurements to reconstruct the momentum.

In general, missing energy signals can occur in the Standard Model when we produce a weak boson decaying as $W \to \ell\nu$ (such as are often produced when a top quark decays) or $Z \to \nu\bar{\nu}$ along with a jet. It also can occur because of mismeasurements of jet energies, which can create an imbalance in apparent transverse energy, even when there is none in reality. In theories beyond the SM, we find missing energy in theories containing dark matter which can be produced at the LHC (i.e.[19] for some studies in the context of effective field theories), including in cascade decays of other particles such as SUSY or UED;[20] in theories with large extra dimensions,[21] where a KK graviton can be produced which escapes from our brane world; or any signal whose decays produce W or Z bosons.

To learn about events with missing energy, let's start with the process

$$pp \to W \to \ell\nu \tag{61}$$

where the W can be of either charge, and the charged lepton ℓ can be any flavor and will match that charge. When we move to the partonic cross sections, at leading order we will have a $q\bar{q}'$ initial state. If we could measure all of the particles involved, this process is very much like producing $Z \to e^+e^-$: the invariant mass of the neutrino and lepton will reconstruct something close to the W mass. However, since we can't detect the neutrino, in practice things are a little complicated.

We know that the initial state had no momentum transverse to the beam (the $\hat{x}$ and $\hat{y}$ directions), and the initial partons had some net boost (which at the LHC was probably pointed in the quark direction for the same reasons discussed above) relative to the lab frame. At the same time, we can measure all three momentum components of the charged lepton, as well as any extra hard jets that may occur in a particular event. Using momentum conservation, we infer the $\hat{x}$ and $\hat{y}$ components of the neutrino momentum:

$$\vec{p}_T^{\,\nu} = -\vec{p}_T^{\,\ell} - \sum_{\text{jets}} \vec{p}_T^{\,\text{jet}} \tag{62}$$

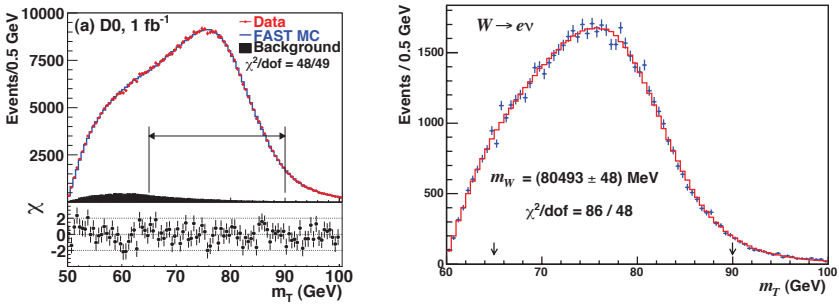

Fig. 14. Transverse mass of W boson as measured by D0 (left) and CDF (right).[23]

where the notation $\vec{q}_T$ reminds us that $\vec{q}_T$ is a vector whose non-zero components are only along the $\hat{x}$ and $\hat{y}$ axes.[j] In practice, we can generalize this definition to include the transverse components of any particle I can measure in the final state: electrons, muons, jets (including b and τ-originated jets), and photons, and the missing transverse momentum is the sum of all of the particles we are unable to detect.

The $\hat{z}$ component of the neutrino momentum cannot be determined this way, because we don't know the boost of the partons along that axis for a particular event. Even if we are pretty sure that the missing energy is actually a neutrino (and not, say, a WIMP, whose mass we don't know a priori and may not be able to ignore), we also can't reconstruct E_ν, because we are missing p_z^ν.

While the missing component of the neutrino momentum means we can't uniquely reconstruct the kinematics of the event, we can make do with what we have. We introduce the transverse energy of the neutrino, which is defined to be just the part of the energy we *can* reconstruct, $E_T^f \equiv |\vec{p}_T^{\,f}|$ for the particle f, which we have assumed is massless. The transverse mass is defined as,

$$M_T \equiv \sqrt{\left(E_T^\nu + E_T^\ell\right)^2 - (\vec{p}_T^{\,\nu} + \vec{p}_T^{\,\ell})^2}\ . \tag{63}$$

It is easy to show that for a $\ell\nu$ pair produced from an on-shell W decay, $M_T \leq M_W$. There is a kinematic edge in the M_T distribution which is used at Fermilab to measure the W mass, and is currently the world's most precise measurement.[23]

[j]Transverse projections are not completely trivial. A nice (and readable) guide can be found in.[22]

The Dark Secrets of the Terascale Downloaded from www.worldscientific.com by MONASH UNIVERSITY on 04/16/16. For personal use only.

Sometimes we are pretty sure there was one missing neutrino in an event, and can use kinematic relations to reconstruct the kinematics. For example, if we are sure that a neutrino came from $W \to \ell\nu$ decay (perhaps because we see evidence that the W itself came from a top decay, and we reconstruct the remainder of the event including some b-tags), we can use the fact that we expect the W to be approximately on-shell to reconstruct the neutrino. If we define its energy as a function of the unknown p_z (and inferred p_x and p_y), $E_\nu(p_z) = \sqrt{p_x^2 + p_y^2 + p_z^2}$, we can approximate,

$$M_W^2 \simeq (p_\ell + p_\nu)^2 = 2p_\ell \cdot p_\nu = 2\left(E_\ell E_\nu(p_z) - \vec{p}_\ell \cdot \vec{p}_\nu\right) \ . \tag{64}$$

This equation is quadratic in p_z, and thus typically yields two solutions. Sometimes, one (or both) of them will be unphysical, and can be discarded, but in general there will be two, and both could describe the actual kinematics. In the case where the W boson itself arises from a top decay, $t \to Wb$, we could combine both solutions with the ℓ and the b-jet and use the one which results in the top closer to being on-shell

7. Outlook

Colliders are currently our most precise probe of short distance physics. The next few years will see large increases in the LHC integrated luminosity, and will allow us to probe increasingly rarer processes and higher energies. Tools such as understanding of collinear behavior, parton distribution functions, and carefully chosen variables will be essential to tease the new physics from the background and ultimately understand what it is. Putting simple tools such as these together can result in very sophisticated analysis of collider data, and will be a lot of the fun of seeing what the LHC tells us!

The Dark Secrets of the Terascale Downloaded from www.worldscientific.com by MONASH UNIVERSITY on 04/16/16. For personal use only.

Acknowledgements

TT would like to acknowledge the excellent organization by Goran and the local team, and partial support from the NSF through grant PHY-0970171 during the time in which these lectures were written. LTW would like to thank Konstantin Matchev, Tim Tait, and the local organizers of TASI 2011 for the invitation, and support.

References

1. T. Han, arXiv:hep-ph/0508097.
2. T. Plehn, arXiv:0810.2281 [hep-ph].

The Dark Secrets of the Terascale Downloaded from www.worldscientific.com by MONASH UNIVERSITY on 04/16/16. For personal use only.

3. M. Perelstein, arXiv:1002.0274 [hep-ph].
4. *et al.* [ALEPH Collaboration], arXiv:1012.2367 [hep-ex].
5. C. Amsler *et al.* [Particle Data Group], Phys. Lett. B **667**, 1 (2008).
6. T. M. P. Tait, *Prepared for Theoretical and Advanced Study Institute in Elementary Particle Physics (TASI 08: The Dawn of the LHC Era), Boulder, Colorado, 2-27 Jun 2008*. Since I never posted these on the arxiv, you can find them on the web: `http://hep.ps.uci.edu/ tait/tait-TASI08.pdf`
7. [ALEPH Collaboration and DELPHI Collaboration and L3 Collaboration and], Phys. Rept. **427**, 257 (2006) [arXiv:hep-ex/0509008].
8. T. Sjostrand, S. Mrenna and P. Z. Skands, Comput. Phys. Commun. **178**, 852 (2008) [arXiv:0710.3820 [hep-ph]].
9. G. Corcella *et al.*, arXiv:hep-ph/0210213.
10. M. Cacciari, arXiv:hep-ph/0607071.
11. A. D. Martin, W. J. Stirling, R. S. Thorne and G. Watt, Eur. Phys. J. C **63**, 189 (2009) [arXiv:0901.0002 [hep-ph]].
12. P. M. Nadolsky *et al.*, Phys. Rev. D **78**, 013004 (2008) [arXiv:0802.0007 [hep-ph]].
13. M. Fairbairn, A. C. Kraan, D. A. Milstead, T. Sjostrand, P. Z. Skands and T. Sloan, Phys. Rept. **438**, 1 (2007) [arXiv:hep-ph/0611040].
14. A. Leike, Phys. Rept. **317**, 143 (1999) [arXiv:hep-ph/9805494].
15. J. L. Hewett and T. G. Rizzo, Phys. Rept. **183**, 193 (1989).
16. P. Langacker, Rev. Mod. Phys. **81**, 1199 (2009) [arXiv:0801.1345 [hep-ph]].
17. M. S. Carena, A. Daleo, B. A. Dobrescu and T. M. P. Tait, Phys. Rev. D **70**, 093009 (2004) [arXiv:hep-ph/0408098].
18. F. Petriello and S. Quackenbush, Phys. Rev. D **77**, 115004 (2008) [arXiv:0801.4389 [hep-ph]].
19. M. Beltran, D. Hooper, E. W. Kolb, Z. A. C. Krusberg and T. M. P. Tait, JHEP **1009**, 037 (2010) [arXiv:1002.4137 [hep-ph]]; J. Goodman, M. Ibe, A. Rajaraman, W. Shepherd, T. M. P. Tait and H. B. P. Yu, Phys. Lett. B **695**, 185 (2011) [arXiv:1005.1286 [hep-ph]]; Y. Bai, P. J. Fox and R. Harnik, JHEP **1012**, 048 (2010) [arXiv:1005.3797 [hep-ph]]; J. Goodman, M. Ibe, A. Rajaraman, W. Shepherd, T. M. P. Tait and H. B. P. Yu, Phys. Rev. D **82**, 116010 (2010) [arXiv:1008.1783 [hep-ph]].
20. T. Appelquist, H. C. Cheng and B. A. Dobrescu, Phys. Rev. D **64**, 035002 (2001) [arXiv:hep-ph/0012100].
21. N. Arkani-Hamed, S. Dimopoulos and G. R. Dvali, Phys. Lett. B **429**, 263 (1998) [arXiv:hep-ph/9803315].
22. A. J. Barr, T. J. Khoo, P. Konar, K. Kong, C. G. Lester, K. T. Matchev and M. Park, arXiv:1105.2977 [hep-ph].
23. M. P. Sanders [For the D0 and CDF Collaborations], arXiv:1009.2903 [hep-ex].
24. C. G. Lester and D. J. Summers, Phys. Lett. B **463**, 99 (1999) [arXiv:hep-ph/9906349].
25. A. J. Barr, B. Gripaios and C. G. Lester, JHEP **0802**, 014 (2008) [arXiv:0711.4008 [hep-ph]].